Evaluation of Stemflow Effects on the Spatial Distribution of Soil Moisture Using TDR Monitoring and an Infiltration Model

IR7685

Evaluation of Stemflow Effects on the Spatial Distribution of Soil Moisture Using TDR Monitoring and an Infiltration Model

Davide Canone[1], Maurizio Previati[2], Stefano Ferraris[3]

[1] Interuniversity Department of Regional and Urban Studies and Planning (DIST), Polytechnic University of Turin, viale Mattioli, 39, 10125 Turin, Italy; Corresponding author: Davide Canone, davide.canone@unito.it

[2] Interuniversity Department of Regional and Urban Studies and Planning (DIST), Polytechnic University of Turin, viale Mattioli, 39, 10125 Turin, Italy;

[3] Interuniversity Department of Regional and Urban Studies and Planning (DIST), Polytechnic University of Turin, viale Mattioli, 39, 10125 Turin, Italy;

ABSTRACT

The partitioning of crop canopy water may affect the soil water distribution and this may in turn affect the sprinkler irrigation application efficiency.

The aim of this work was to develop a methodology to evaluate the spatial and temporal soil water content distribution in the case of sprinkler irrigation application efficiency considering stemflow.

Time domain reflectometry (TDR) soil moisture monitoring was carried out on eight soil water sensor locations for both center pivot and traveling big gun irrigation in different phenological and tillage cases. The two case studies were chosen because they show the two opposite limits of the application of the methodology.

Two water distribution estimation methods were employed: the raw measured soil moisture and

the model simulation of the infiltration process. The infiltration process were modeled by means of the two dimensional (2D) Richard's equation. The simulations were calibrated on the data measured at eight soil water sensor locations. The stemflow and surface runoff conveyed in the inter-row by hilling were obtained as additional model fitting parameters.

During center pivot irrigation, 34% of the water delivered in the interrow was conveyed in the row. During the travelling big gun irrigation, 88% of the water delivered in the row was conveyed in the interrow.

Soil water distributions calculated from measured data overestimated the irrigation application efficiency by approximately 15%. The spatial and temporal soil water content distribution obtained from simulation of water infiltration process allowed the mass balance closure in both case studies.

The proposed simulation method evaluates stemflow effects on the water distribution profile, leading to accurate application efficiency calculations.

INTRODUCTION

Several studies have reported an increase in air temperatures in northern Italy (Brunetti et al., 2006; Ciccarelli et al., 2008 Corti et al., 2009). Climate change is expected to further increase air temperature, thereby intensifying water scarcity and irrigation requirements in the Mediterranean region (IPCC, 2007; Goubanova and Li, 2007; Rodriguez Diaz et al., 2007).

In most Mediterranean countries, the agricultural sector is the major user of water resources, for both irrigated farming and livestock (OECD, 2006). The expected air temperature increase due to climate change will further increase the water demand from the agricultural sector. As a consequence, an increase in groundwater drawdown and water diversion from rivers is expected.

The excessive groundwater drawdown and the minimum acceptable discharge of rivers are becoming topical issues. To comply with diversion restrictions, an optimal management of water resources at the farm level is needed, especially in view of increasing water demands, limited resources, and aquifer contamination (Kumar and Singh, 2003).

In the scenario described above, mitigation of climate change may have significant positive effects (Fischer et al., 2007). The most efficient and affordable irrigation technique must be chosen so that water consumption is optimized, and the necessary soil water stock for crop requirements is guaranteed (Facchi et al., 2004). The complex phenomena occurring in the soil of the plains have to be simulated in detail, in order to compute such soil water stock (e.g., Canone et al., 2015; Baudena et al., 2012). To obtain the required water savings, it is also important to perform the irrigations properly and to choose the right irrigation scheduling so that the optimal water distribution in soil is achieved (Rodriguez-Sinobas et al., 2016).

The way that water redistribution occurs in the soil after irrigation should be routinely analyzed in order to improve application efficiency. In sprinkler irrigation, the water is partitioned by the crop canopy into stemflow, throughfall, and interception storage. Stemflow is the water conveyed from the leaves to the stem, where it flows down to the soil. Throughfall is the water that falls on the soil surface directly or indirectly through the leaves. Interception storage is the amount of water that temporally remains on the plant. It will evaporate directly from leaves.

Several studies have examined such processes under either natural rainfall or sprinkler systems (van Wesenbeeck and Kachanoski, 1988; van Wesenbeeck et al., 1988; Lamm and Manges, 2000; Li and Rao, 2000; Paltineanu and Starr, 2000).

In their studies, van Wesenbeeck and Kachanoski (1988) and van Wesenbeeck et al. (1988) reported evidence of the importance of water partitioning by the crop canopy to determine spatial

patterns of soil water content. In their studies of the spatial and temporal dynamics of soil water content in the surface tilled layer, they performed soil water content measurements on a transect perpendicular to corn rows, using 20 cm vertical TDR probes to obtain daily measurements for the entire growing season. During the growing season, they found a higher rainfall infiltration in the row position, which was attributed to stemflow. They also found higher drying rates at row positions that were related to the influence of the crop roots. Their results showed that the preferential infiltration and drying along the row cause higher temporal variance of the soil moisture below the row compared to soil moisture below the interrow.

Lamm and Manges (2000) focused their study on water partitioning by the corn canopy under sprinkler irrigation performed with one high-pressure impact sprinkler system and one low-pressure spray system. They also considered water partitioning by the crop canopy during rain events. They reported a correlation between the partitioning of sprinkler irrigation and rain when water was delivered above the canopies. Stemflow increased when the spray heads were positioned within the canopy at 2.2 m above the ground. Lamm and Manges (2000) developed a method for predicting the stemflow and throughfall components of water partitioning by the crop canopy. They found that the stemflow amount decreased linearly with plant spacing and increased linearly with irrigation amount, whereas throughfall amount increased linearly with both plant spacing and irrigation amount. They reported an average stemflow of 53%, but the stemflow varied of 16% among rows.

Li and Rao (2000) studied the effect of the winter wheat (*Tricticum aestivum* L.) canopy on sprinkler irrigation water partitioning. The authors collected the water above the canopy and the throughfall below the canopy with catch cans located at 0.85 m above the ground and on the ground surface. Li and Rao (2000) also found that stemflow increased with increasing irrigation amounts.

They found that stemflow was not significantly influenced by sprinkler uniformity.

Paltineanu and Starr (2000) studied the partitioning of water by the corn canopy under rainfall and traveling big gun sprinkler irrigation. They found positive linear relationships for both stemflow and throughfall to rainfalls and sprinkler irrigation events intensities. Paltineanu and Starr (2000) measured soil water content with four capacitance sensor probes at row and interrow positions at 10 minutes intervals. Their work focused on the analysis of soil water infiltration under tillage and no-tillage treatments. They found higher infiltration in the no-tillage row position for rainfall events with intensities less than 15 mm.

The irrigation water canopy partitioning influences the water distribution patterns in the soil. Different techniques for the description of soil water distribution profiles were proposed and tested by several authors (Timlin et al. 2001; Bruckler et al. 2004; Fernández-Gálvez et al. 2006). Soil water distribution patterns can be determined by interpolation techniques as reported by Fernández-Gálvez et al. (2006). They measured soil water content on a 5-hectare experimental site. They performed the measurements along twelve profiles located along three 15 m transects. The profiles were 5 m apart, and the measurements were recorded at seven depths from 0.03 m to 1.00 m, at 30 minutes intervals. Moreover, they performed occasional measurements at six depths from 0.10 m to 1.00 m at thirty-one sites. They evaluated some interpolation techniques as tools for estimating soil water profiles from point measurements. They observed that large errors can affect the estimation of the water content profile when it is based on soil water content measurements at few depths using sensors with very limited sampling volumes. They observed that such errors can be reduced by using a vertical interpolation technique. However, their technique was tested on large profiles (5 m) including several rows, and it involved occasional measurements of the detailed vertical profile.

Timlin et al. (2001) studied water partitioning by the soybean (*Glicine max* L.) canopy and water redistribution in the row-interrow profile. They measured the soil water content down to the depth of 40 cm with TDR vertical probes at hourly intervals. They leveled the soil at the measurement site in order to minimize surface topography effects on runoff and infiltration. They also found patterns of water distribution determined by stemflow, which were not always in agreement with those found by van Wesenbeeck and Kachanoski (1988) and van Wesenbeeck et al. (1988). Timlin et al. (2001) found higher soil water content at row position in one plot, whereas in another plot, they found higher soil water content in the interrow position. They ascribed the different soil water content patterns to either the spatial variability of soil water content vs. matric potential relationship or soil compaction. Their results suggest that, to model the water movement in row crops, it is important to use an accurate 2D simulation of soil water processes and to account for the canopy effect.

Bruckler et al. (2004) modeled the root uptake and infiltration process under the corn canopy taking into account stemflow effects on water supply homogeneity. They employed a 2D matric potential model, which assumes soil layers with different hydrodynamic properties in the vertical direction and a homogeneous soil in the horizontal direction. Their model was calibrated on matric potential measurements performed with automatic tensiometers at ten different depths between 0.10 m and 1.50 m. The measurements were performed at 15 minutes intervals. The results of their work provided a description of the water distribution in the root soil layer, but they neglected the possible water runoff caused by the wavy microtopography related to earthing up practices.

The first aim of this work was to develop and experimentally test a methodology for the evaluation of sprinkler irrigation application efficiency that considers stemflow influences on soil water distribution patterns. The effects of stemflow were also evaluated by considering surface runoff.

In order to investigate such influences, soil water content measurements were performed and water distribution patterns were estimated. However, a sufficiently detailed TDR water content spatial distribution measurement is not achievable with TDR systems suitable for routine soil water content monitoring, which may provide dataset useful to farmers for irrigation efficiency estimation. Therefore, the second objective is to develop a new technique for the estimation of water distribution profiles. The soil water distribution measured over eight points for each irrigation was interpolated by means of three techniques: the employment of the raw measured water contents, the spline interpolation of the measured water contents and the simulation of the water infiltration process.

MATERIALS AND METHODS

Irrigation monitoring, data interpolation and simulation of the water infiltration process

During the measurement campaigns, two corn sprinkler irrigation events were monitored. The measurement campaigns were performed in two farms located in the plain of the Cuneo district (Piedmont, Italy). In both farms the corn was planted in 75 cm rows and the measurement campaigns were performed during the flowering growth stage. The soils of the two farms belong respectively to the *sandy-loam* (Farm 1) and *silty-loam* (Farm 2) textural classes. In Table 1, we report the percentages of the particle size classes for each soil sample collected and the sampling depth. The irrigation methods examined were a center pivot system that irrigates 5.06 ha (Farm 1) and a travelling big gun system that irrigates 2.65 ha (Farm 2). The examined fields had different microtopography. The field irrigated by center pivot was flat whereas the field irrigated by travelling big gun had a wavy microtopography, where the soil surface along the corn rows was more elevated than along the inter-rows. The wavy microtopography was generated by the farmer,

who hilled up the corn in May. Measurements were carried out during irrigation events performed by the farmers following their usual practices. Measurements were carried out to define the following parameters: i) the total field irrigation water depth; ii) the time duration of each irrigation event; and iii) the water depth stored in the soil root layer.

To evaluate the irrigation water depth delivered during the irrigation events, four rain gages were installed on the fields above the corn canopy. Soil water content measurements were carried out using a device composed by: one TDR cable tester (Tektronix Metallic Cable Tester 1502C manufactured by Tektronix Inc., Beaverton, OR, USA) connected to a notebook and a multiplexer, which allowed automatic measurements of soil moisture at eight points along the soil profile at 5 minutes intervals. The TDR signals were sampled and acquired using the WinTDR software (Or et al., 2004). Volumetric soil water content θ (m^3 m^{-3}) was computed using the composite dielectric approach described by Roth et al. (1990). TDR probes were 150 mm long, and they were made with three stainless steel rods held by a nylon spacer. All connections were made by RG58 50 Ω coaxial cables.

A few days after sowing, before the spring rainy period, the probes were horizontally inserted into the soil at depths of 0.05, 0.15, 0.25, and 0.40 m for the center pivot monitoring and at depths of 0.05, 0.15, 0.30, and 0.50 m for the travelling big gun monitoring (Figure 1). After two months, during the flowering growth stage, the soil water content was measured allowing consolidation of soil. The probe depths were chosen to monitor the entire root zone depth. The soil depths in the two examined fields were limited by layers of stones located at 0.5 and 0.65 m depth, respectively. The probes were placed in two different locations below the row and the interrow, to obtain two data sets for each measurement site.

The employment of a greater number of probes is not advisable, because the system would become

both too expensive for routine measurements carried out by farmers associations and too slow for simultaneous measurements across the profile. In order to obtain a detailed description of the water content distribution, the raw measured soil moisture values, the interpolation of measured data and a simulation method were tested.

In the interpolation method, the spline technique was employed to interpolate the measured values at the beginning of the irrigation and at the end of the monitoring. The soil water content distribution along the row - interrow vertical profile was estimated on a square grid with cells of 1 by 1 cm by using the thin plate spline as described by Wahba (1990). Thin plate spline is a physically based interpolation scheme for arbitrarily spaced tabulated data. It is classified as a deterministic interpolation technique with a local stochastic component. This interpolation technique is relatively simple to implement since it does not require any assumption on the spatial covariance of the data. Instead, kriging and kriging-based interpolation methods require a correct calibration of a semivariogram (Cressie 1991; Huisman, 2002; Wackernagel, 1995). The spline interpolation only requires a smoothing parameter which regulates the trade-off between the closeness of the function to the data and the smoothness of the function.

In the simulation method, the finite volume ADHYDRA code (Manzini and Ferraris, 2004) was employed to simulate the infiltration process. This code simulates the two-dimensional infiltration process by solving the Richard's equation on a grid 0.37 m width and 0.5 or 0.65 m deep, which in our work was set up as a square grid with cells of 1 by 1 cm. A width of the grid of 0.37 m was chosen because it is the distance between the row and the inter-row. The horizontal grid size was assumed as half row spacing because the center of the interrow was considered as the center of a symmetric domain. The water content output was recorded also on a square grid of 1 by 1 cm. The horizontal grid size stays within the length scale proposed by Lehmann and Or (2009) and Or *et*

al. (2015) for the applicability of the Richards equation for lateral capillary flow.

The initial conditions were given by the water content measurements performed at the beginning of the irrigation as explained in paragraph 2.3.1, whereas the boundary conditions were as follows:

- Two constant fluxes were imposed on the surface boundary. The stemflow flux was imposed on the first ten centimeters horizontally taken from the center of the row. The residual flux was imposed on the remaining surface.
- A no flux condition was imposed on the vertical boundaries because of the symmetry.
- A no flux condition was imposed on the bottom boundary.

The ratio between the two constant fluxes delivered into the row (stemflow) and into the interrow (throughfall and surface runoff) was treated as a fitting parameter for the infiltration model. The simulations were calibrated on data measured at eight control points. The control points were represented by the locations of the TDR probes. The simulations were initialized by running them for thirty minutes without any water input.

Determination of soil water retention and hydraulic conductivity parameters

In this study, the van Genuchten equation (1980) (Eq. 1) and the Brooks and Corey relation (1964) (Eq. 2) were chosen as water retention and hydraulic conductivity models, respectively:

$$\frac{\left(\theta-\theta_{\mathrm{r}}\right)}{\left(\theta_{\mathrm{S}}-\theta_{\mathrm{r}}\right)}=\left[1+\left(\frac{h}{h_{\mathrm{g}}}\right)^{n}\right]^{-m}, \tag{1}$$

$$\frac{K\left(\theta\right)}{K_{s}}=\left(\frac{\theta-\theta_{r}}{\theta_{S}-\theta_{r}}\right)^{\eta} \tag{2}$$

where n [-] and m [-] are two shape parameters of the water retention function, η [-] is the shape parameter of the hydraulic conductivity function, h is the matric potential [L], h_g is the matric

potential scale parameter for the relation of water retention of van Genuchten (1980), expressed as height of the water column [L], θ_S is the volumetric soil water content at field saturation [L^3L^{-3}], θ_i is the initial volumetric soil water content [L^3L^{-3}], θ_r is the residual water content [L^3L^{-3}], K_S is the saturated hydraulic conductivity [LT^{-1}], and K is the hydraulic conductivity of the soil in unsaturated conditions [LT^{-1}]. The m and n depend on soil texture and are related through the equation:

$$m = 1 - \frac{k_m}{n} \text{ with } n > k_m, \tag{3}$$

where the parameter k_m is a user index (Haverkamp *et al.*, 2005; Leij et al., 2005). The user index k_m= 1 corresponds to the conductivity model of Mualem (1976), whereas k_m = 2 gives the conductivity model of Burdine (1953). In this study, the model of Mualem (1976) was chosen.

The pressure scale parameter h_g and the water content scale parameters θ_r and θ_S depend on soil structure (Haverkamp et al., 2002). The parameter θ_r may be associated with the immobile water held (by adsorptive forces) within in a dry soil profile. In practice however, its value is generally estimated by fitting the water retention equation to measured data points reducing θ_r to an empirical fitting parameter valid for the range of data points used. For this reason, in this study, its value was set equal to zero, θ_r = 0, as proposed by various authors, (e.g., Kool et al., 1987; van Genuchten et al., 1991; Leij et al., 1996). The shape parameters m and n were calculated from the particle size cumulated distribution curve as follow.

Similar to the θ (h) van Genuchten equation, the cumulated particle size distribution curve, $F_p(d_p)$, is represented by an S-shaped unimodal function (Haverkamp and Reggiani, 2002):

$$F_{\mathrm{p}}\left(d_{\mathrm{p}}\right) = \left[1 + \left(\frac{d_{\mathrm{pg}}}{d_{\mathrm{p}}} \right)^{N} \right]^{-M} \tag{4}$$

where M [-] and N [-] are the shape parameters of the cumulated distribution curve related through:

$$M = 1 - \frac{k_M}{N} \text{ with } N > k_M \tag{5}$$

where k_M takes values of 1 or 2 as explained for k_m, d_p [L] is the diameter of particles, and d_{pg} [L] is a particle size scale parameter defined by fitting in the interval $0 < d_{pg} \leq 2$ mm.

The water retention curve can be characterized by only one shape index independently from the chosen equation (i.e., Brooks and Corey, 1964; van Genuchten, 1980) as demonstrated by Haverkamp et al. (2005) and Leij et al. (2005). The shape index is defined as "Shl_{wr}" and for the van Genuchten (1980) equation is given by:

$$Shl_{wr} = \frac{m_0 n_0}{1 + m_0} = \frac{m_0 n_0 \left(k_m + m_0 n_0\right)}{k_m + 2 m_0 n_0}, \tag{6}$$

where the subscript "0" indicates $\theta_r = 0$ and k_m is given as in Eq. (3).

A shape index for the particle size cumulated distribution curve (Shl_{ps}) can be expressed similar to the Shl_{wr}, employing the principle of shape similitude between the water retention curve and the cumulated particle size distribution curve (Haverkamp and Parlange, 1986). The Shl_{ps} is then given by:

$$Shl_{ps} = \frac{MN\left(k_M + MN\right)}{k_M + 2MN} \tag{7}$$

where k_M is given by Eq. (5).

The two shape parameters are related through Eq. (8) (Haverkamp et al., 2006):

$$Shl_{ps} = Shl_{wr}\left(1 + \gamma_S\right) \tag{8}$$

where γ_s is a tortuosity coefficient defined as a function of the fractal index f_d (Fuentes et al., 1998):

$$\gamma_s = \frac{2 f_d - 1}{2 f_d \left[1 - f_d\right]} \tag{9}$$

The fractal index is equal to one third of the fractal dimension and is defined as a function of

porosity ε_p [L^3 L^{-3}] by (Fuentes et al., 1998):

$$(1-\varepsilon_p)^{f_d} + \varepsilon_p^{2 f_d} = 1 \tag{10}$$

The shape parameters (*m* and *n*) of the water retention curve were derived from the value of the water retention shape index considering the positive root of Eq. (6) for *m*, and deriving *n* from *m* by Mualem (1976) conditions as described in Lassabatère et al. (2006).

$$m = \frac{1}{S_{hlwr}}\left(\sqrt{1+S_{hlwr}^2} - 1\right) \tag{11}$$

$$n = \frac{1}{1-m} \tag{12}$$

$$\eta = \frac{2}{\lambda} + 2 + p \tag{13}$$

where λ is the product of $m \times n$ and p is 0.5 for Mualem (1976) conditions.

Scale parameters K_S and h_g were obtained by fitting on the observed water content data. Two K_S values were obtained separately for the row and the interrow soil profiles to account for the varying degree of soil compaction. Finally, the scale parameter θ_S was estimated by TDR measurement after the irrigation event.

Estimation of water content distribution

In this work, three techniques for the description of the water distribution patterns were employed.

Measured data

Water distribution in the root layer profile was described by means of the measured data. The row-interrow soil profile (width 0.37 m) was divided into eight rectangular cells (width 0.185 m), each

one corresponding to a TDR probe. Four cells were located below the row and four below the interrow. TDR data were related to the thickness of each cell (Figure 2), to obtain the water depth stored in it: i.e., below the row the value obtained by the probe placed at a depth of 0.05 m was considered representative of the cell between depths of 0 m and 0.10 m. In the same way, the soil water content value obtained by the 0.15 m depth probe was considered representative of the cell between depths of 0.10 m and 0.225 m, the soil water content value obtained by the 0.30 m depth probe was considered representative of the cell between depths of 0.225 m and 0.400 m and the soil water content value obtained by the 0.50 m depth probe was considered representative of the cell between depths of 0.400 m and 0.650 m. The same method was employed below the interrow. The water distribution in the soil profile was calculated at three times (t_0, t_1 and t_2). The time t_0 corresponds to the beginning of the irrigation event, t_1 corresponds at the end of the irrigation event, and t_2 is the time at which the redistribution became so low that the evapotranspiration effects on the water distribution patterns were considered to be not negligible.

Spline interpolation of measured data

In order to estimate the soil water storage, the row – interrow profile (Figure 1) was subdivided in 5 by 5 cm square cells. The water content obtained by spline interpolation of TDR data was related to the thickness of each cell in order to obtain the water depth stored in it, and the water distribution in the soil profile was calculated at t_0, t_1 and t_2.

Simulation of the infiltration process

The soil water content values obtained by simulation of the infiltration process were related to the height of the 5 by 5 cm cells. The water distribution in the soil profile was calculated at t_0, t_1 and t_2.

Soil water distribution in the soil profile at time t_1 was calculated to monitor the infiltrated water

depth at the end of the irrigation. According to this procedure, the depth of water stored within a cell at time t_i (St_i) is given by:

$$St_{jk}(t_i) = \theta_{jk}(t_i) \cdot l_k \quad (14)$$

where θ_i [L^3L^{-3}] is the soil water content assigned to the considered cell at time t_i (Figure 2). The subscript j ($1 \leq j \leq p$) indicates the assumed cell along the horizontal axis perpendicular to the corn row, and p[-] is the number of cells along the horizontal axis. The subscript k ($1 \leq k \leq q$) indicates the considered cell along the vertical axis, q [-] is the number of cells along the vertical axis, and l [L] is the thickness of the considered cell.

In order to evaluate the performance of the simulation in comparison with measured data, the standard error was calculated according to the relation:

$$Se = \frac{\sqrt{\frac{1}{n}\sum_{i=1}^{n}\left(\theta_{sjk}^2 - \theta_m^2\right)}}{\sqrt{n}} \quad (15)$$

where θs is the soil water content obtained by the simulation of the infiltration process and θm is the correspondent soil water content value measured by the TDR probe defined according to Figure 1.

Efficiency calculation

The field water application efficiency, defined by Kruse et al. (1990) as the average depth of water stored in the root zone divided by the average depth of water applied to a field, P [L], is given by:

$$E_{ax} = \frac{\sum_{j=1}^{q}\sum_{k=1}^{r} St_{2\,jk} - \sum_{j=1}^{q}\sum_{k=1}^{r} St_{0\,jk}}{P} \quad (16)$$

where the "x" subscript is an index of the method employed to estimate the soil water content distribution. The x is replaced by "m" to indicate an estimation based only on measured soil

water content values, by "*i*" to indicate an estimation based on spline interpolation of measured soil water content values and by "*s*" to indicate an estimation based on results of the simulation of infiltration process.

RESULTS AND DISCUSSION

In this section, the results of the stemflow effect evaluation on water distribution and irrigation efficiency are presented and discussed. The presentation of results follows the scheme of the methodologies applied: experimental monitoring, assessment of water distribution by means of soil water content measured data, spline interpolation, and assessment of water distribution by means of the simulation of the water infiltration process.

The efficiency terms in the presentation and the discussion of results and conclusions will be followed respectively by the subscript "*m*" to indicate an estimation based only on measured data, by the subscript "*i*" to indicate an estimation based on spline interpolation of measured data, and by the subscript "*s*" to indicate an estimation based on simulation results.

Experimental monitoring of stemflow effects on water infiltration and redistribution

This section reports the results obtained by the TDR irrigation monitoring. The results of the TDR monitoring were employed as input for both the spline interpolation and for the calibration of the infiltration model.

During the pivot irrigation, a water depth of about 30 mm was distributed in 40 minutes. Figure 3 shows the water content measured by the TDR probes during the time in which the water was delivered and during water redistribution after the end of the irrigation events. An analysis of the data recorded below the row during the pivot irrigation event (Figure 3a) shows that the water content registered by the TDR probes at the end of the irrigation event, starting from the surface

of the soil, are 0.321, 0.292, 0.218 and 0.098 m^3m^{-3}. The maximum soil water content registered can be considered as corresponding to the field saturation, because it corresponds to the saturation of 80% of soil porosity (ε = 0.400). In fact, this value is the lower limit of the normal range of the interval of soil water content at field saturation ($\theta_{FS} \approx 0.8 \div 0.9\ \varepsilon$). The minimum soil water content increase after the irrigation event was registered by the deepest probe (0.019 m^3m^{-3}). Thirty minutes after the irrigation system was stopped, the first three probes from soil surface measured a water content reduction of 0.051, 0.046 and 0.009 m^3m^{-3}, while the deepest probe registered a slight increase (0.009 m^3m^{-3}). The soil water content variation registered by the two deepest probes, after the irrigation system was stopped, is negligible. The analysis of the water content measurements suggests an horizontal distribution of water in direction of the inter-row. Such hypothesis is supported by the fact that there were no evidences of stemflow runoff to the interrow (depletion of water at the soil surface), and the TDR probes recorded a reduction of water storage below the corn row with a negligible soil water content increase at the bottom of the profile.

The interrow TDR probes set (Figure 3b) registered an increase of water content only in the surface layer, where, during the water delivery, the water content increased from 0.126 m^3m^{-3} to 0.299 m^3m^{-3}. Since there were no evidences of stemflow runoff to the interrow, the observed increase was due to the throughfall directly infiltrated in the center of the interrow. The throughfall in the center of the interrow generated a vertical flow from surface that did not reach the probe located at 15 cm depth. Since the probe located at 15 cm depth did not record increase in soil water content, the probe location was neither reached by the vertical infiltration flux nor by the horizontal redistribution flux. Therefore, the lack of water content increase below a depth of 0.15 m means that the horizontal redistribution of water from the center of the row did not reach the center of the interrow.

During the thirty minutes after the irrigation system was stopped, at the center of the interrow, the probe at 0.05 m depth registered a water content reduction of 0.019 m^3m^{-3}, the probe at 0.15 m depth registered a water content increase of 0.005 m^3m^{-3}. Since a very low variation of soil water content was recorded by the two probes located near the soil surface and the deepest probes did not register any water content change, it is possible to say that the water dropped in the center of the interrow was maintained in the first two layers of the soil without any flow toward the deeper layers.

The above considerations imply that half an hour after the irrigation system was stopped, the soil water content could not be considered constant on the horizontal axis perpendicular to the corn rows. Horizontal water fluxes determined by matric potential gradients were still present, whereas vertical water fluxes, responsible for deep percolation losses, were negligible.

At the end of the measurements, the water distribution in the profile and consequently the water depth stored could not be reliably estimated using only the eight measured water content values. In fact, the soil water content between the two sets of probes could reasonably be lower than the water content measured below the corn row. In such conditions, if the water content registered below the corn row could have been attributed to one half of the profile, the result could have been an overestimation of the stored water depth and application efficiency.

To evaluate the error to which a wrong estimate of water distribution can lead, the mass balance was computed on the data measured during an irrigation performed by pivot (E_{am}). Therefore, the water content registered by each probe at the beginning of the irrigation (t_0) and thirty minutes after the end of the irrigation (t_2) were considered. The water content was converted to water depth over the examined profile. The water depth measured in each cell before and after the irrigation event was employed in Eq. (14) and Eq. (16) to compute mass balance. The results of the

application efficiency estimation based only on the TDR monitoring of the center pivot irrigation event are physically unacceptable (E_{am} = 112.3%). The error in the efficiency estimation is marginally due to an error in the water content measurement. The standard error on water content estimation is comprised between 0.010 m^3m^{-3} and 0.020 m^3m^{-3} as reported by Topp et al. (1980) and Or and Wrigth (2000). The error is mainly due to the representation of the water distribution on eight cells. Such representation cannot take in account the correct distribution of water in the space between the row and the inter-row. As a matter of fact, the standard error between the soil water content distribution estimated by direct measurement at eight point and that obtained by the simulation of the infiltration process is 0.034 m^3m^{-3}, which is almost the double of the magnitude of the error expected by measurements campaigns performed by TDR. The error in the efficiency estimation highlight the need for either a higher resolution in water content data obtainable by an interpolation method or a simulation of the infiltration process.

The results of the TDR monitoring during the irrigation performed by the travelling big gun are shown in Figure 4. The initial water contents measured below the row were lower than those measured below the interrow. The initial water contents were high compared to pivot measurements. Their values ranged between 0.109 m^3m^{-3} and 0.219 m^3m^{-3} below the row and between 0.194 m^3m^{-3} and 0.285 m^3m^{-3} below the interrow.

The maximum water content registered within the soil profile was achieved below the interrow at 90 minutes after the irrigation system was stopped. The first three probes from the soil surface below the interrow measured water content values greater than the 80% of porosity (ε = 0.420) corresponding to field saturation ($\theta > 0.8\ \varepsilon$), whereas below the row, only the probe at 0.15 m measured a water content corresponding to field saturation.

The comparative analysis of the soil water content values measured when the irrigation system

was stopped (t_1) and those measured 90 minutes later (t_2) showed an increase of water depth stored in the profile after the water delivery was interrupted. The water storage was due to surface ponding caused by the high irrigation intensity generated by the travelling big gun and the field microtopography. In fact, the ridges made in May determined a wavy shape of the field surface in the direction perpendicular to the corn rows.

The field microtopography determined localized water ponding and a consequent increase in the water depth infiltrated in the interrow, which was partially redistributed towards the row. In fact, the TDR monitoring (Figure 4) registered higher water contents below the interrow, at t_2 the water content at depths of 0.05, 0.15 and 0.30 m reached values of 0.378, 0.344 and 0.343 m^3m^{-3}, respectively, whereas the probes set below the row registered lower water contents. The probes at depths of 0.05, 0.15 and 0.30 m below the row registered an increase of water content between t_1 and t_2. The increase in water content below the row was due to the horizontal redistribution of water from the saturated interrow profile. Both TDR probes located at a depth of 0.5 m showed no increase in soil water content. The results of the monitoring performed during the travelling big gun irrigation event showed an inverse behavior compared to the pivot irrigation (Figure 3). The travelling big gun monitoring shows a slightly higher increase in water depth storage below the interrow.

Because water content at the bottom of the profile did not increase below the row or below the interrow, results suggest that no water loss by deep percolation occurred. As for the previous case, the water mass balance was calculated on the root zone water storage obtained from measured data. It did not agree with the evidence of no deep percolation given by the TDR measurements (E_{am} = 88.8%). The standard error between the soil water content distribution obtained by the measured data and that obtained by the simulation of the infiltration process is 0.039 m^3m^{-3}, which

is the double of the magnitude of the error expected for soil water content measurements by TDR. The analysis of TDR data shows heterogeneity of water content distribution along the horizontal axis perpendicular to corn rows. To evaluate the effect of the heterogeneity of water content distribution and the discrepancy between the E_{am} and the expected absence of deep percolation**,** the soil water contents measured at t_0, t_1 and t_2 were interpolated using the thin plate spline, and the infiltration process was simulated using the ADHYDRA code as for the pivot irrigation.

Estimation of water distribution patterns by using the thin plate spline

The thin plate spline interpolation was performed in order to estimate the water distribution pattern in the row-interrow profile. Soil water content measurements by TDR (Table 2 and 3) were interpolated. The results of interpolation are shown in Figures 5 and 6. Figure 5 shows the results of soil water content interpolation at t_0, t_1 and t_2 during center pivot irrigation. The water distribution patterns are generally acceptable, but a detailed analysis reveals some results that unlikely represent the real distribution of soil water content. The interpolation generates water content values lower than 0.050 m^3m^{-3}, which is the lowest measured water content. At t_0, one of the areas with lowest water content value is located between depths of 0.25 m (θ = 0.055 m^3m^{-3}) and 0.40 m (θ = 0.050 m^3m^{-3}). There is no physical explanation for such low water content in this area. The water distribution patterns generated by thin spline generally underestimate the soil water content below a depth of 0.4 m, where the values are extrapolated. Such underestimation is more evident in the plots concerning t_1 and t_2, where the bottom of the soil profile looks drier than it was at before the input of water (t_0). The thin spline overestimates soil water content in the layer between the soil surface and a depth of 0.05 m due to extrapolation from data measured at 0.05 m depth. The overestimation of soil water content is more evident at t_1 and t_2. The thin spline method was employed because it is simple and can be applied to few data, but it has only one adjustable

smoothing parameter. As a consequence, the errors in water content estimation cannot be controlled by the interpolation procedure.

The water content distribution patterns were converted to water depth over the examined profile and employed in Eq. (14) and Eq. (16), as explained in section "Estimation of water content distribution", to calculate the application efficiency based on interpolation results (E_{ai}). The E_{ai} value (101.3%) shows that the estimation of the water distribution patterns obtained by interpolation is better than that obtained directly by measured data, because it leads to an efficiency value closer to 100% than the E_{am} value (88.8%), but it is still unacceptable, because the E_{ai} value is greater than 100%.

Figure 6 shows the results of soil water content interpolation at t_0, t_1 and t_2 during traveling big gun irrigation. The water distribution patterns show several inconsistencies with their change in time and some unlikely results. At t_0, an area with low soil water content is located around the value measured at a depth of 0.30 m below the row. The drier area is wider at a depth between 0.30 and 0.50 m, where a higher soil water content was measured. The drier area should be located at a depth between 0.15 and 0.30 m. The thin spline method overestimates the soil water content below a depth of 0.50 m, where the values were obtained by extrapolation. The overestimation is more evident below the interrow, where the soil water content achieves field saturation values at the bottom of the profile.

At t_1, the water distribution pattern is not related to the irrigation process. The water distribution is given by an area of increasing soil water content centered at the driest point, which is located at a depth of 0.3 m below the row. The water distribution pattern at t_1 gives soil water content values at the bottom of the soil profile that are lower than those obtained at t_0. In fact, the maximum soil water content values below a depth of 0.05 m at t_1 are in the range of 0.250 to 0.300 m^3m^{-3} below

the row and in the range of 0.300 to 0.350 m^3m^{-3} below the interrow. The water distribution pattern at t_1 is not consistent with the infiltration of part of the water delivered in the time interval between t_0 and t_1.

At t_2, the water distribution pattern between the soil surface and a depth of 0.5 m is consistent with the water infiltration process. At the bottom of the profile, the thin spline method slightly overestimates the soil water content. The soil water content at the bottom of the soil profile decrease during the infiltration process and achieve the lowest value below the inter-row. The position of the lowest value of soil water content at the bottom of the soil profile is not consistent with the infiltration process that is more intense in the interrow, neither it is consistent with the distribution patterns at t_1 and at t_2.

As for the previous case, the water application efficiency was calculated on the water storage of the root zone obtained from interpolated data. The E_{ai} value (70.1%) was even lower than the E_{am} (88.8%) value. The E_{ai} value did not agree with the evidence of no deep percolation, as shown by the TDR measurements.

The thin spline interpolation of soil water content values measured during the center pivot and traveling big gun sprinkler irrigation was not always consistent with the infiltration process, and such inconsistencies were not predictable or adjustable by interpolation parameters.

Estimation of water distribution patterns by simulation of the infiltration process

The simulation of the water infiltration process was performed in order to estimate the water distribution pattern in the row – interrow profile. The initial conditions were given by the initial water contents measured by TDR (Table 2 and 3).

Simulations' results were validated by using water content data. The water content differences between simulated and measured values are reported in Table 2 and Table 3 and displayed in

Figures 3 and 4.

Figure 3 shows the comparison between results of the measurements and simulation of the infiltration process during center pivot irrigation. The figure shows that the model barely follows the measured data during rapid transients of imbibition and that it reaches water content values very close to the measured ones when the redistribution process takes place.

The results of the simulation of the infiltration during the pivot irrigation are presented in Figure 7, where the water content at each node of the lateral boundaries of the grid, from depths of 0.05 m down to 0.5 m, is plotted versus time (at time intervals of 5 minutes).

The simulation was stopped at the same time the monitoring was terminated (t_2). The differences between the simulated and the measured data were calculated at t_1 and t_2. The differences (Table 2) show a good agreement between the model results and the measured data at t_2. The mean difference in absolute value between the model and the measured values at t_1 and t_2 were respectively 0.013 m^3m^{-3} and 0.010 m^3m^{-3}. In some locations, the differences were either lower or similar to the instrumental resolution of the Tektronix 1502C, which is 0.004 m^3m^{-3} (Hook and Livingston, 1996). Such small differences could not be displayed by the instrument so they must be considered as negligible.

The simulation results reported in Figure 5 show abrupt steps of soil water content between the row and the interrow at t_0 and at t_1. The soil water content steps are determined by the different hydraulic conductivity values assigned to the row and interrow soils, which are influenced by wheel traffic (e.g. Boulal et al., 2010). The water distribution patterns obtained by the simulation of the infiltration process are more detailed than those obtained directly by measured soil water content values. The water distribution patterns obtained by the simulation were always consistent with the infiltration process, and local estimation errors determined by the interpolation process

are avoided.

A comparison between the results of the TDR monitoring of the travelling big gun irrigation and the results of the simulation of the infiltration process is given in Figure 4. In figure 8, the results of the simulation of the infiltration process at both sides of the grid were plotted versus time (at time intervals of 5 minutes).

The simulation barely followed the measured water contents during rapid transients of imbibition, but it reached water content values similar to the measured data when the redistribution process slowed down. The simulation was stopped at t_2, and the differences between the simulated and measured data were calculated at t_1 and t_2. The differences (Table 3) show a strong agreement between the model results and the measured data at the end of the simulation. The mean difference in absolute value between the simulation and the measured data at t_1 and t_2 were respectively 0.022 m^3m^{-3} and 0.013 m^3m^{-3}. The simulation results generally overestimated the soil water content below the interrow and underestimated it in the row.

The simulation results reported in Figure 6 show abrupt steps of soil water content more evident than those observed in the case of center pivot irrigation. In fact, the soil water content steps are still observable at t_2. In spite of the water content steps, the water distribution patterns obtained by the simulation of the water infiltration process were more detailed than those obtained directly by the soil water content measured data. The former were always consistent with the infiltration process, and the unpredictable soil water content estimation errors determined by interpolation were avoided. Moreover, the simulation method allows for the estimation of the stemflow.

Estimation of the stemflow from the water distribution in the soil profile

The estimation of water partitioning by the corn canopy was obtained as fitting a parameter. The ratio between stemflow and throughfall fluxes imposed as boundary conditions on the surface

boundary let vary to fit the results of the simulation of the infiltration process onto water content measured data. The value of the parameter was estimated while minimizing the RMSE between simulated and measured data. The lowest RMSE found for the center pivot irrigation corresponds to one third of the inflow water depth infiltrated in the interrow and two thirds infiltrated in the row.

According to the partitioning results, the water depth delivered on the row is 34% greater than what should be expected if stemflow did not occur. The stemflow values obtained from the simulation of the infiltration process under center pivot irrigation are similar to those reported by Parkin and Codling (1990), which ranged between 27 and 50%, but were much lower than the values between 50 and 60% reported by van Wesenbeeck and Kachanoski (1988). The low stemflow value is due to the canopy architecture. In fact, the measurements were done during the third week of July, when the aged corn canopies have a reduced capacity to convey water along the stem.

The partitioning obtained from the simulation of the infiltration process under the travelling big gun irrigation cannot be considered as an estimation of stemflow and throughfall. In fact, the surface runoff caused by the wavy microtopography, generated by the farmer's soil managing practices (section "Irrigation monitoring, data interpolation and simulation of the water infiltration process"), conveyed most of the water toward the interrow. The lowest RMSE found corresponds to the water partitioning of 94% infiltrated in the interrow and 6% infiltrated in the row. According to the partition results, the depth of water delivered on the interrow is 88% greater than what should be expected if microtopography did not play a role. The technique for the estimation of water distribution in soil profiles proposed in this work allowed the estimation of water partitioning between the row and the interrow. The proposed technique can also take in account heterogeneous

distribution of water at the soil surface caused by stem flow and field microtopography.

Estimation of the application efficiency

All the water contents obtained at the end of the simulation were used in Eq. (14) and Eq. (16), as explained in section "Estimation of water content distribution", to calculate the application efficiency based on simulation results (E_{as}). The E_{as} value is physically acceptable and consistent with the soil water content measured at the bottom of the examined profile. In fact, in the case of the center pivot irrigation, the water content increments registered at the end of the monitoring by the two probes located at a depth of 0.4 m were 2.7% below the row and 0% below the interrow. The very low increments of water content at the bottom of the profile indicate a negligible deep percolation water loss, which leads to an high application efficiency (99%).

The E_{as} value calculated for the travelling big gun irrigation (99.5%) is much higher than the result of the E_{am} (88.8%). The data collected by the TDR probes on the two sides of the profile did not allow a good estimation of the water distribution in the central part of the profile, which led to the underestimation of the water application efficiency. The value of E_{as} consistent with the water increments registered by the TDR probes at the bottom of the profile. In fact, the registered increments of 0.9% below the row and 0% below the interrow suggest no water loss by deep percolation. The E_{as} values show, in both cases, the importance of an infiltration model for the estimation of the water distribution patterns to calculating the water mass balance.

CONCLUSIONS

In this study, monitoring of soil water content profiles was carried out during two irrigation events to evaluate the sprinkler irrigation mass balance considering the stemflow influence on water distribution profiles. The two irrigation events were performed using center pivot and travelling

big gun sprinkler irrigation systems, respectively.

Measured data, thin spline interpolation and a 2D simulation of the infiltration process performed by means of a Richards equation code were tested, to develop a new technique for the estimation of water distribution profiles. Field-scale soil hydraulic parameters were derived from TDR water content measurements and soil particle size analysis. These parameters were used as inputs to simulate the two-dimensional water infiltration process. Saturated hydraulic conductivity and the irrigation water partitioning between row and interrow were treated as model fitting parameters. Simulation results were validated on eight control points represented by the TDR soil volumetric water content measurements.

The results of TDR monitoring of the irrigation events highlighted the need for a higher resolution in water content data obtainable either by more soil water sensors, interpolation method or by the simulation of the infiltration process. The thin spline interpolation results were not always consistent with the infiltration process, and such inconsistencies were not predictable and adjustable by interpolation parameters. The comparison among observed water content, interpolated water content data and the calibrated ADHYDRA simulations showed that the software is able to correctly reproduce the water spatial distribution in the row – interrow soil profile. Such detailed infiltration simulations allowed us to calculate the water mass balance accounting for the effects of stemflow caused by the corn canopy and surface runoff caused by microtopography.

The center pivot and the travelling big gun irrigation systems showed two opposite behaviors: the first with the higher water intake on the row, due to stemflow effect; the second with the higher water intake on the interrow. In the latter case, stemflow effects were reversed due to the limited infiltration rate and field microtopography, causing surface runoff that conveyed the water toward

the interrow. The water application efficiency was calculated from the water content values estimated over the soil profile by the simulation of the infiltration process between the row and in the interrow. The mass balance calculated on the refined water content distribution were approximately 99% in both cases.

Our work showed that it is not advisable to calculate water mass balance based only on soil water measurements if the infiltration rate is highly variable over the field surface. In such cases, we recommend the determination of soil hydraulic parameters to perform detailed water infiltration simulations and to refine the estimation of the actual water distribution patterns.

ACKNOWLEDGMENTS

This study was partially funded by the Italian Ministry of Research through Italian Research Project of Relevant Interest (PRIN2010-2011), prot. 20104ALME4, "National network for monitoring, modelling, and sustainable management of erosion processes in agricultural land and hilly-mountainous area" (PI Mario Aristide Lenzi) and through the project PRIN2010-11 "New methodologies for water resources management in hydro-climatic uncertainty scenarios" (PI Alberto Bellin).

REFERENCES

Baudena, M., Bevilacqua, I., Canone, D., Ferraris, S., Previati, M., and Provenzale, A. (2012). Soil water dynamics at a midlatitude test site: Field measurements and box modeling approaches. *J Hydrol*, 10.1016/j.jhydrol.2011.11.009, 414–415, 329-340.

Boulal, H., Mateos, L., and Gómez-Macpherson, H. (2010). Soil management and traffic effects on infiltration of irrigation water applied using sprinklers. *Irrig Sci*., 10.1007/s00271-010-0245-1, 29(5), 403-412.

Brooks, R.H., and Corey, A.T. (1964). Hydraulic properties of porous media. *Hydrology Paper 3,* Colorado State University, Fort Collins, Colorado, USA.

Bruckler, L., Lafolie, F., Doussan, C., and Bussières, F. (2004). Modeling soil-root water transport with non-uniform water supply and heterogeneous root distribution. *Plant Soil*, 10.1023/B:PLSO.0000030187.33135.b8, 260(1), 205-224.

Brunetti, M., Maugeri, M., Monti, F., and Nanni, T. (2006). Temperature and precipitation variability in Italy in the last two centuries from homogenised instrumental time series. *Int J Climatol*, 26(3), 345-381

Burdine, N.T. (1953). Relative permeability calculation from pore size distribution data. *Petr Trans Am Inst Min Metall Eng*, 198, 71-77.

Canone, D., Previati, M., Bevilacqua, I., Salvai, L., and Ferraris, S. (2012). Field measurements based model for surface irrigation efficiencyassessment. *Agr Water Manage*, 10.1016/j.agwat.2015.03.015, 156, 30-42.

Ciccarelli, N., von Hardenberg, J., Provenzale, A., Ronchi, C., Vargiu, A., and Pelosini, R. (2008). Climate variability in North-Western Italy during the second half of the 20th century. *Glob Planet Change*, 63, 185-195.

Corti, S., Decesari, S., Fierli, F., Fuzzi, S., Provenzale, A., Sabbioni, C., Santoleri, R., and Vitale, V. (2009). Clima, cambiamenti climatici globali e loro impatto sul territorio nazionale. Provenzale A (ed) Quaderni dell'ISAC 1. ISAC-CNR, Bologna, Italy. ISBN: 978-88-903028-0-0

Cressie, N.A.C. (1991). *Statistics for Spatial Data*. John Wiley & Sons, New York, NY, USA

Facchi, A., Ortuani, B., Maggi, D., and Gandolfi, C. (2004). *Coupled SVAT–groundwater model for water resources simulation in irrigated alluvial plains*. *Environmental Modelling & Software, Integrated Catchment Modelling and Decision Support*, 10.1016/j.envsoft.2003.11.008, 19(11), 1053-1063.

Fernández-Gálvez, J., Simmonds, L.P., and Barahona, E. (2006). Estimating detailed soil water profile

records from point measurements. *Eur J Soil Sci*, 10.1111/j.1365-2389.2005.00761.x, 57(5), 708-718.

Fischer, G., Tubiello, F.N., van Velthuizen, H., Wiberg, D.A. (2007). Climate change impacts on irrigation water requirements: Effects of mitigation, 1990–2080. *Technol Forecast Soc*, 10.1016/j.techfore.2006.05.021, 74, 1083-1107

Fuentes, C., Vauclin, M., Parlange, J.-Y., and Haverkamp, R. (1998). Soil water conductivity of a fractal soil. In: Baveye, P., Parlange, J.-Y., and Stewart, B. (eds), Fractals in Soil Science. CRC Press, Boca Raton, Florida, USA..

Goubanova, K., Li, L. (2007). Extremes in temperature and precipitation around the Mediterranean basin in an ensemble of future climate scenario simulations. *Glob Planet Change*, 57(12), 27-42.

Haverkamp, R., and Parlange, J.-Y. (1986). Predicting the water-retention curve from a particle-size distribution: 1. Sandy soils without organic matter. *Soil Sci*, 142, 325-339.

Haverkamp, R., and Reggiani, P. (2002). Physically based water retention prediction models. In: Dane, J.H., and Topp, G.C. (eds), Methods of soil analysis: Part 4-Physical Methods. SSSA Book Ser 5. Soil Science Society of America, Madison, Wisconsin, USA.

Haverkamp, R., Reggiani, P., and Nimmo, J.R. (2002). Property-transfer models. In: Dane, J.H., and Topp, G.C. (eds), *Methods of soil analysis: Part 4-Physical Methods*, SSSA Book Ser 5, Soil Science Society of America, Madison, Wisconsin, USA.

Haverkamp, R., Leij, F.J., Fuentes, C., Sciortino, A., and Ross, P.J. (2005). Soil water retention: I. Introduction of a shape index. *Soil Sci Soc Am J*, 69, 1881-1890.

Haverkamp, R., Debionne, S., Viallet, P., Angulo-Jaramillo, R., and de Condappa, D. (2006). Soil Properties and Moisture Movement in the Unsaturated Zone. In: Delleur, J.W. (ed), *Handbook of Groundwater Engineering, 2nd edn*., CRC Press Boca Raton, Florida, USA.

Hook, W.R., and Livingston, N.J. (1996). Errors in converting time domain reflectometry measurements of propagation velocity to estimates of soil water content. *Soil Sci Soc Am J*, 60, **35-41.**

Huisman, J.A., Snepvangers, J.J.J.C., Bouten, W., and Heuvelink, G.B.M. (2002). Mapping spatial variation in surface soil water content: comparison of ground-penetrating radar and time domain reflectometry. ***J Hydrol*****, 10.1016/S0022-1694(02)00239-1,269(3-4), 194-207.**

IPCC. (2007). Climate change 2007: The physical science basis—summary for policymakers. ***Contribution of WGI to the 4th Assessment Report of the IPCC*****, Geneva, Switzerland.**

Kool, J.B., and Parker, J.C. (1987). Development and evaluation of closed-form expressions for hysteretic soil hydraulic-properties. ***Water Resour Res*****,** 23, **105-114.**

Kruse, E.G., Bucks, D.A., and von Bemuth, R.D. (1990). Comparison of irrigation systems. In: Stewart, B.A., and Nielsen, D.R. (eds), ***Irrigation of Agricultural Crops Agron Monogr No 30,*** **Am Soc Agron, Madison, pp 475-508.**

Kumar, R., and Singh, J. (2003). Regional water management modelling for decision support in irrigated agriculture. ***J Irrig Drain Eng*****, 129, 432-439.**

Lamm, F.R., and Manges, H.L. (2000). Partitioning of Sprinkler Irrigation Water by a Corn Canopy. ***Trans ASAE*****, 43(4), 909-918**

Lassabatère, L., Angulo Jaramillo, R., Soria Ugalde, J.M., Cuenca, R., Braud, I., and Haverkamp, R. (2006). Beerkan estimation of Soil Transfer Parameters trough Infiltration Experiments-BEST. ***Soil Sci Soc Am J*****, 10.2136/sssaj2005.0026, 70, 521-532.**

Lehmann, P., Or, D. (2009). Evaporation and capillary coupling across vertical textural contrasts in porous media. *Physical Review E - Statistical, Nonlinear, and Soft Matter Physics*, 10.1103/PhysRevE.80.046318, 80(4), 046318.

Leij, F.J., Alves, W.J., van Genuchten, M.T., and Williams, J.R. (1996). Unsaturated soil hydraulic database UNSODA 1.0 User's Manual. ***Rep EPA/600/R-96/095*****, US EPA, Ada.**

Leij, F.J., Haverkamp, R., Fuentes, C., Zatarain, F., and Ross, P.J. (2005). Soil water retention: II. Derivation and application of shape index. ***Soil Sci Soc Am J*****, 69, 1891-1901.**

Li, J., and Rao, M. (2000). Sprinkler water distributions as affected by winter wheat canopy. *Irrig Sci*, 20, 29-35.

Manzini, G., and Ferraris, S. (2004). Mass-conservative finite volume methods on 2-D unstructured grids for the Richards' equation. *Adv Water Resour*, 27(12), 1199-1215.

Mualem, Y. (1976). A new model for predicting the hydraulic conductivity of unsaturated porous media. *Water Resour Res*, 12, 513-522.

OECD. (2006). Report on the OECD workshop on agriculture and water: sustainability, markets and policies. OECD, Adelaide, Australia.

Or, D., and Wraith, J.M. (2000). Soil water content and water potential relationships. In: Sumner M.E. (ed), Handbook of Soil Science. CRC Press Boca Raton, Florida, USA, pp A53-A85.

Or, D., Jones, S.B., van Shaar, J.R., Humphries, S., Koberstein, L., 2004. WinTDR Version6. 1 – soil analysis software users guide. USU Soil Physics Group, University of Connecticut and Utah State University.

Or, D., Lehmann, P., Assouline, S. (2015). Natural length scales define the range of applicability of the Richards equation for capillary flows. *Water Resour Res*, 10.1002/2015WR017034, 51, 7130-7144.

Paltineanu, I.C., and Starr, J.L. (2000). Preferential flow through corn canopy and soil water dynamics across rows. *Soil Sci Soc Am J*, 64, 44-54.

Parkin, T.B., and Codling, E.E. (1990). Rainfall distribution under a corn canopy: implication for managing agrochemicals. *Agron J*, 82, 1166-1169.

Rodriguez Diaz, J.A., Weatherhead, E.K., Knox, J.W., and Camacho, E. (2007). Climate change impacts on irrigation water requirements in the Guadalquivir river basin in Spain. *Reg Environ Change*, 7, 149-159.

Rodriguez-Sinobas, L., Provenzano, G., Roldán-Cañas, J. (2016). Water management strategies in irrigated areas. *Agric Water Manage*, 10.1016/j.agwat.2016.02.014 ,170, 1-4.

Roth, K., Schulin, R., Fluehler, H., and Attinger, W. (1990). Calibration of TDR for water content measurement using a composite dielectric approach. *Water Resour Res*, 10.1029/WR026i010p02267, 26(10),

2267-2273.

Soil Survey Laboratory Staff. 1992. Soil survey laboratory methods manual. *Soil Sur-vey Investigations Report n◦42, Version 2.0*. USDA-SCS U.S. Government Printing Office, Washington, DC, USA.

Timlin, D., Pachepsky, Y., and Reddy, V.R. (2001). Soil water dynamics in row and interrow positions in soybean (*Glycine max* L.). *Plant Soil*, 237, 25-35.

Topp, G.C., Davis, J.L., and Annan, A.P. (1980). Electromagnetic determination of soil water content: Measurements in coaxial transmission lines. *Water Resour Res* 16:574–582.

van Genuchten, M.T. (1980). A closed form equation for predicting the hydraulic conductivity of unsaturated soils. *Soil Sci Soc Am J*, 44, 892-898.

van Genuchten, M.T., Leij, F.J., and Yates, S.R. (1991). The RETC Code for quantifying the hydraulic functions of unsaturated soils. *Rep EPA 600/2-91/065*, US EPA, Ada

van Wesenbeeck, I.J., and Kachanoski, R.J. (1988). Spatial and temporal distribution of soil water in the tilled layer under a corn crop. *Soil Sci Soc Am J*, 52, 363-368.

van Wesenbeeck, I.J., Kachanoski, R.J., and Rolston, D.E. (1988). Temporal persistence of spatial patterns of soil water content in the tilled layer under a corn crop. *Soil Sci Soc Am J*, 48, 934-941.

Wackernagel, H. (1995). Multivariate Geostatistics. An introduction with applications. Springer Verlag, Berlin, Germany.

Wahba, G. (1990). Spline Models for Observational Data. SIAM, Philadelphia, Pennsylvania, USA.

FIGURE CAPTIONS

Fig. 1 Sections of the two soil profiles monitored by TDR. The positions of the probes are indicated by dots.

Fig. 2 Scheme of the water distribution in the soil profile described by means of the measured data at t0 in the field irrigated by traveling big gun.

Fig. 3 The plots show the results of the TDR monitoring and the simulation of the infiltration process below the row and the interrow during the center pivot irrigation. Black markers represent TDR measurements and white markers represent ADHYDRA simulated water contents. The duration of the irrigation, from t_0 to t_1 is 40 minutes and the water depth delivered is 30 mm.

Fig. 4 The plots show the results of the TDR monitoring and the simulation of the infiltration process below the row and below the interrow during the traveling big gun irrigation. Black markers represent TDR measurements, and white markers represent ADHYDRA simulated water contents. The duration of the irrigation, from t_0 to t_1 is 90 minutes and the water depth delivered is 65 mm.

Fig. 5 Vertical 2D distribution of soil water content during the center pivot irrigation event before the irrigation (t_0), at the end of the irrigation (t_1), and at the end of the simulation (t_2). Figures (5a-5c) represent the soil water content interpolated by using thin spline method. Figures (5d-5e) represent the soil water content distribution simulated by using the ADHYDRA code.

Fig. 6 Vertical 2D distribution of soil water content during the traveling big gun irrigation event before the irrigation (t_0), at the end of the irrigation (t_1), and at the end of the simulation (t_2). Figures (6a-6c) represent the soil water content interpolated by using thin spline method. Figures (6d-6e) represent the soil water content distribution simulated by using the ADHYDRA code.

Fig. 7 These plots show the results of the ADHYDRA simulation of the water infiltration process during the center pivot irrigation event.

Fig. 8 These plots show the results of the ADHYDRA simulation of the water infiltration process during the traveling big gun irrigation event.

Table 1. Particle size distribution

Farm	Depth [m]	Clay [%]	Fine silt [%]	Coarse silt [%]	Fine sand [%]	Coarse sand [%]
1 *Sandy - loam*	0.10	11.5	18.7	7.8	18.5	43.5
	0.30	10.8	19.6	8.2	19.1	42.3
2 *Silty - loam*	0.05	16.9	29.1	33.4	17.5	3.1
	0.15	18.1	29.7	34.7	14.8	2.7
	0.30	18.1	29	33.2	15.4	4.3
	0.50	25.6	29.6	28.7	13.8	2.3
	0.65	29.5	27.6	26.6	13.3	3

Note: Relative abundances of the particle size classes – defined according to the USDA Classification System (Soil Survey LaboratoryStaff, 1992) – are reported for each soil sample collected along with the sampling depth.

Table 2. Measured soil water content, simulated soil water content and difference between measured and simulated soil water content [m^3m^{-3}] – Center pivot

Depth [m]	t_0		t_2 (measured)		t_2 (simulated)		t_1		t_2	
	row	interrow	row	interrow	row	interrow	row	interrow	row	interrow
0.05	0.096	0.126	0.270	0.280	0.258	0.262	0.004	0.005	-0.013	-0.018
0.15	0.089	0.094	0.250	0.110	0.245	0.095	-0.012	-0.010	-0.005	-0.015
0.25	0.111	0.056	0.210	0.057	0.213	0.056	-0.048	-0.001	0.003	-0.001
0.40	0.079	0.050	0.107	0.051	0.080	0.051	-0.018	-0.003	-0.027	0.000

Note: Soil water content measured at the beginning of the center pivot irrigation (t_0) and at the end of monitoring (t_2). Difference values between the simulated and measured data below the row and the interrow carried out at the end of the irrigation (t_1) and at the end of the simulation (t_2).

Table 3. Measured soil water content, simulated soil water content and difference between measured and simulated soil water content [m^3m^{-3}] – Traveling big gun system

Depth [m]	***t*₀**		***t*₂ (measured)**		***t*₂ (simulated)**		***t*₁**		***t*₂**	
	row	**interrow**	**row**	**interrow**	**row**	**interrow**	**row**	**interrow**	**row**	**interrow**
0.05	0.109	0.194	0.320	0.378	0.333	0.379	0.047	-0.020	0.013	0.000
0.15	0.184	0.259	0.337	0.344	0.323	0.375	-0.024	0.008	-0.014	0.031
0.30	0.164	0.224	0.193	0.343	0.186	0.357	0.000	-0.040	-0.008	0.015
0.50	0.219	0.285	0.227	0.285	0.212	0.293	-0.013	-0.023	-0.015	0.008

Note: Soil water content measured at the beginning of the traveling big gun sprinkler irrigation (*t*₀) and at the end of monitoring (*t*₂). Difference values between the simulated and measured data below the row and the interrow carried out at the end of the irrigation (*t*₁) and at the end of the simulation (*t*₂).

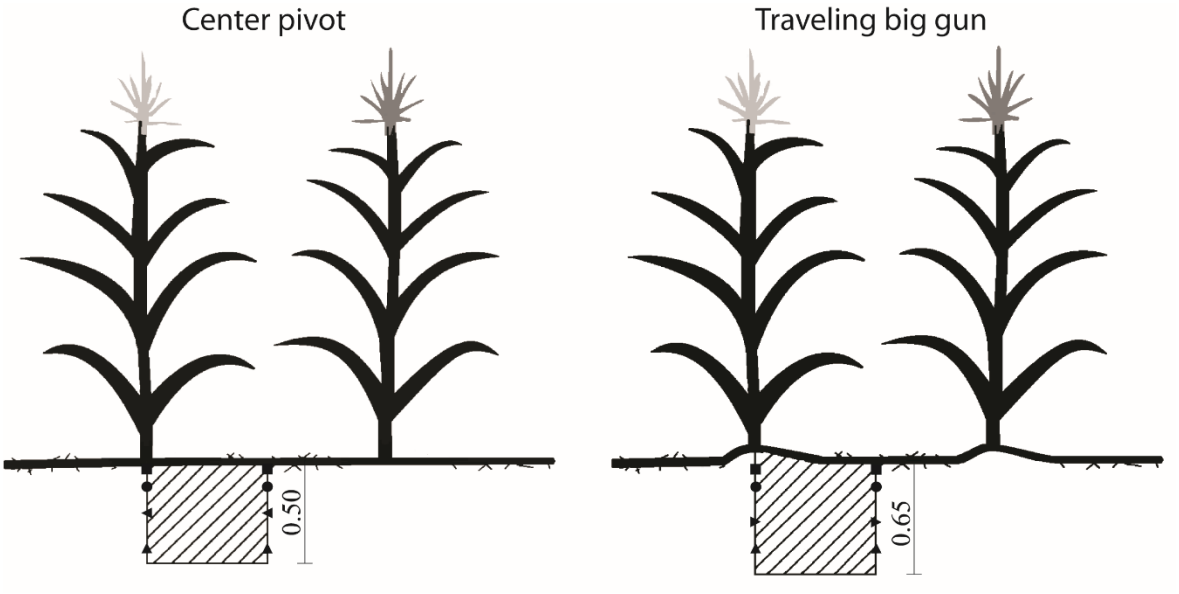

Figure 1

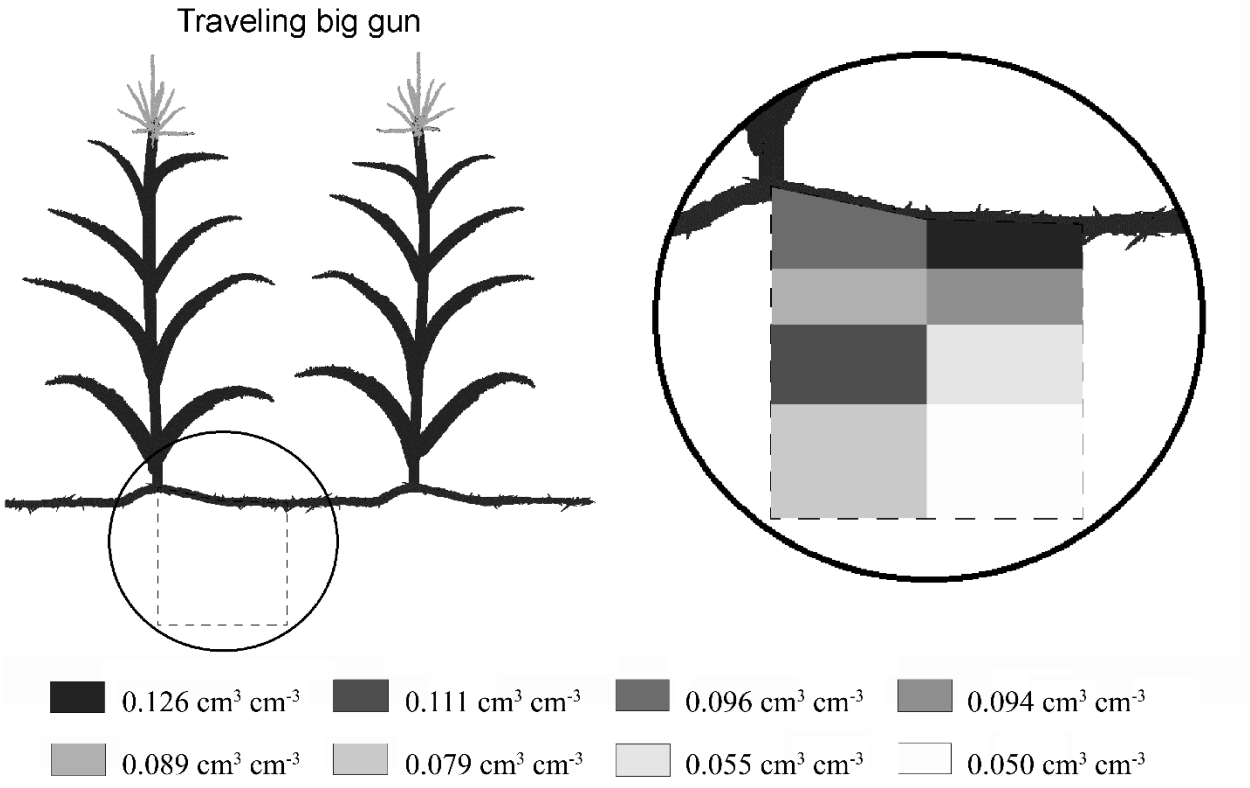

Figure 2

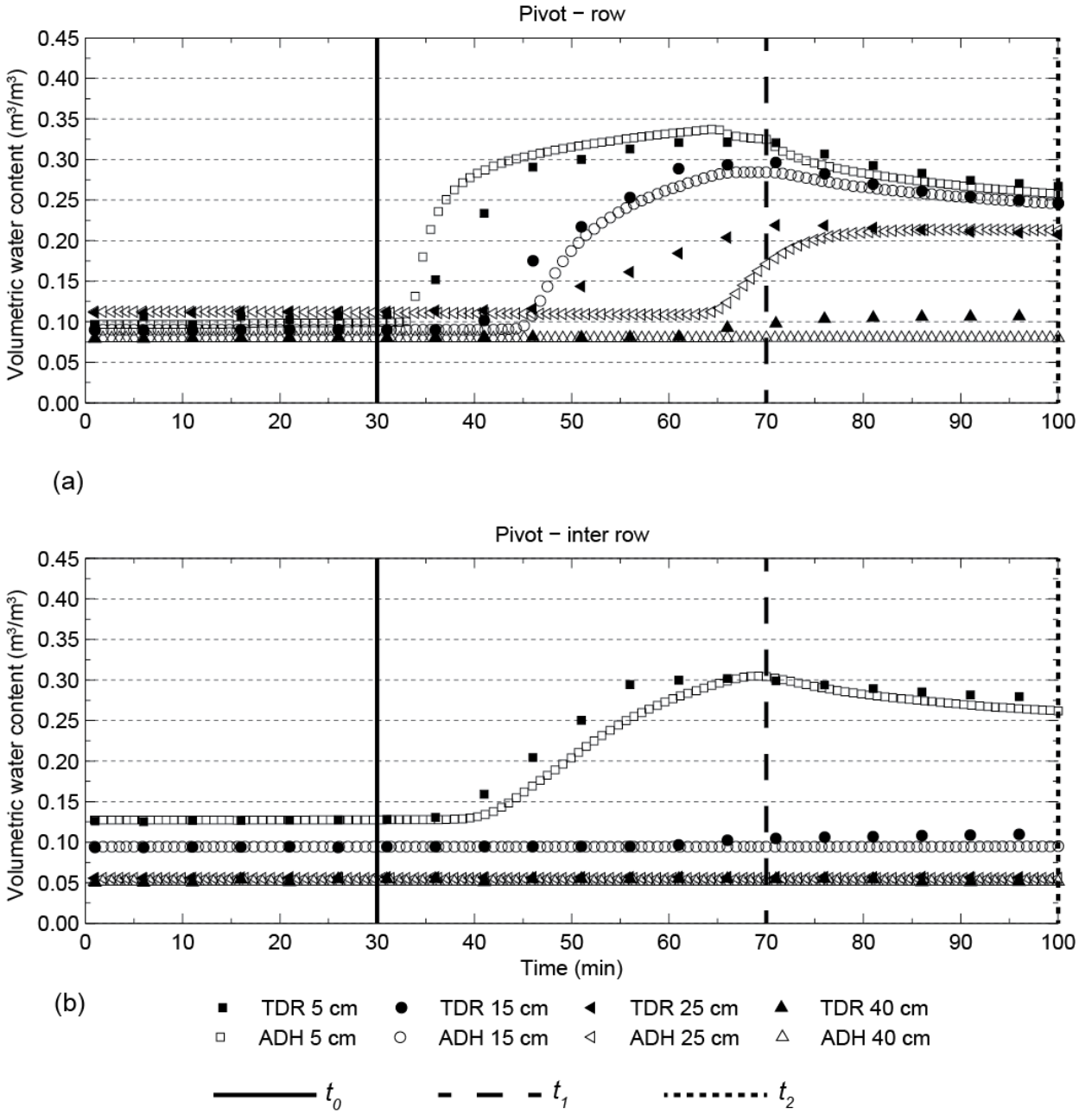
Pivot − row
Volumetric water content (m³/m³)
0.45
0.40
0.35
0.30
0.25
0.20
0.15
0.10
0.05
0.00
0
10
20
30
40
50
60
70
80
90
100
(a)
Pivot − inter row
Volumetric water content (m³/m³)
Time (min)
(b)
TDR 5 cm
TDR 15 cm
TDR 25 cm
TDR 40 cm
ADH 5 cm
ADH 15 cm
ADH 25 cm
ADH 40 cm
t_0
t_1
t_2

Figure 3

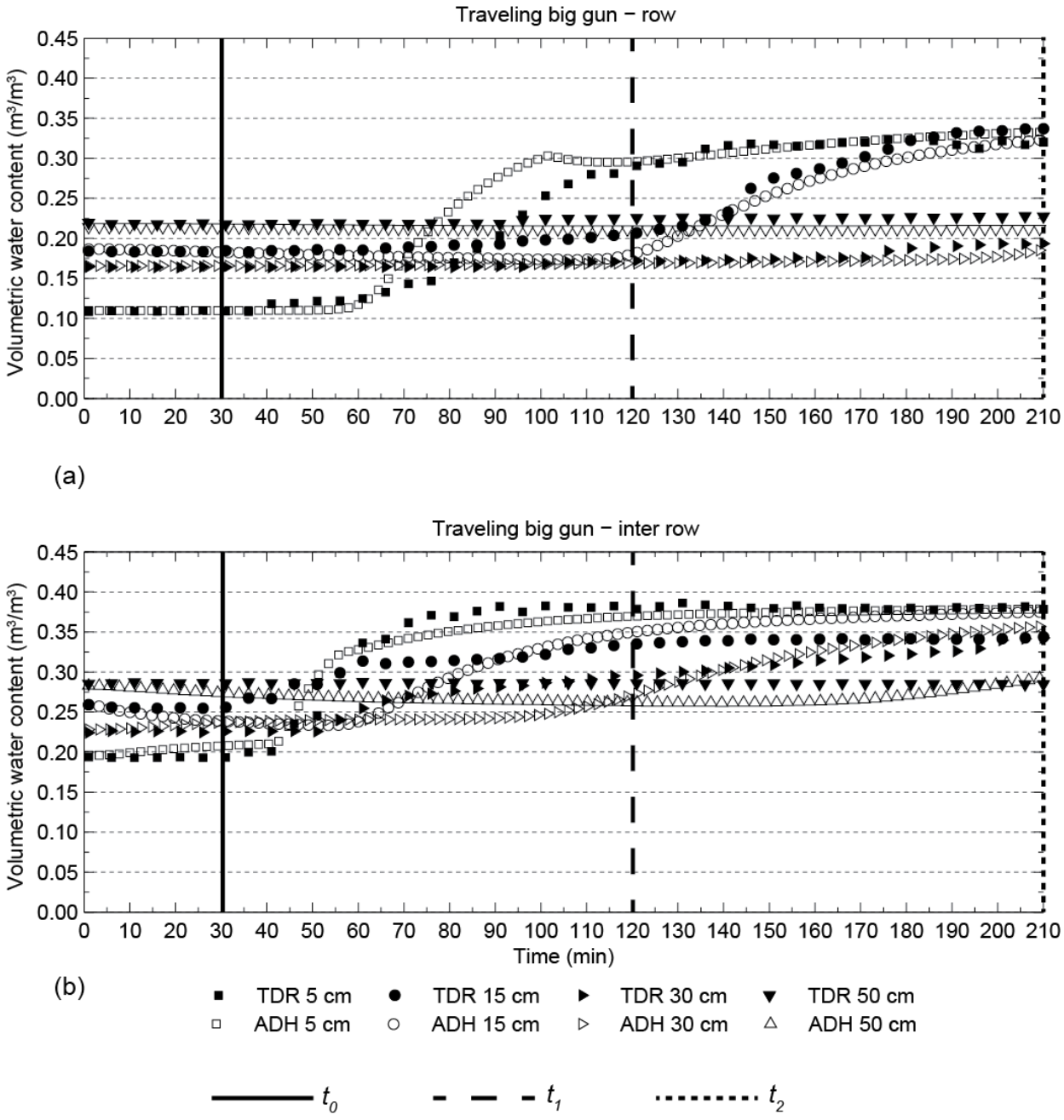
Traveling big gun − row
Volumetric water content (m³/m³)
0.45
0.40
0.35
0.30
0.25
0.20
0.15
0.10
0.05
0.00
0 10 20 30 40 50 60 70 80 90 100 110 120 130 140 150 160 170 180 190 200 210
(a)
Traveling big gun − inter row
Volumetric water content (m³/m³)
Time (min)
(b)
TDR 5 cm
TDR 15 cm
TDR 30 cm
TDR 50 cm
ADH 5 cm
ADH 15 cm
ADH 30 cm
ADH 50 cm
t_0
t_1
t_2

Figure 4

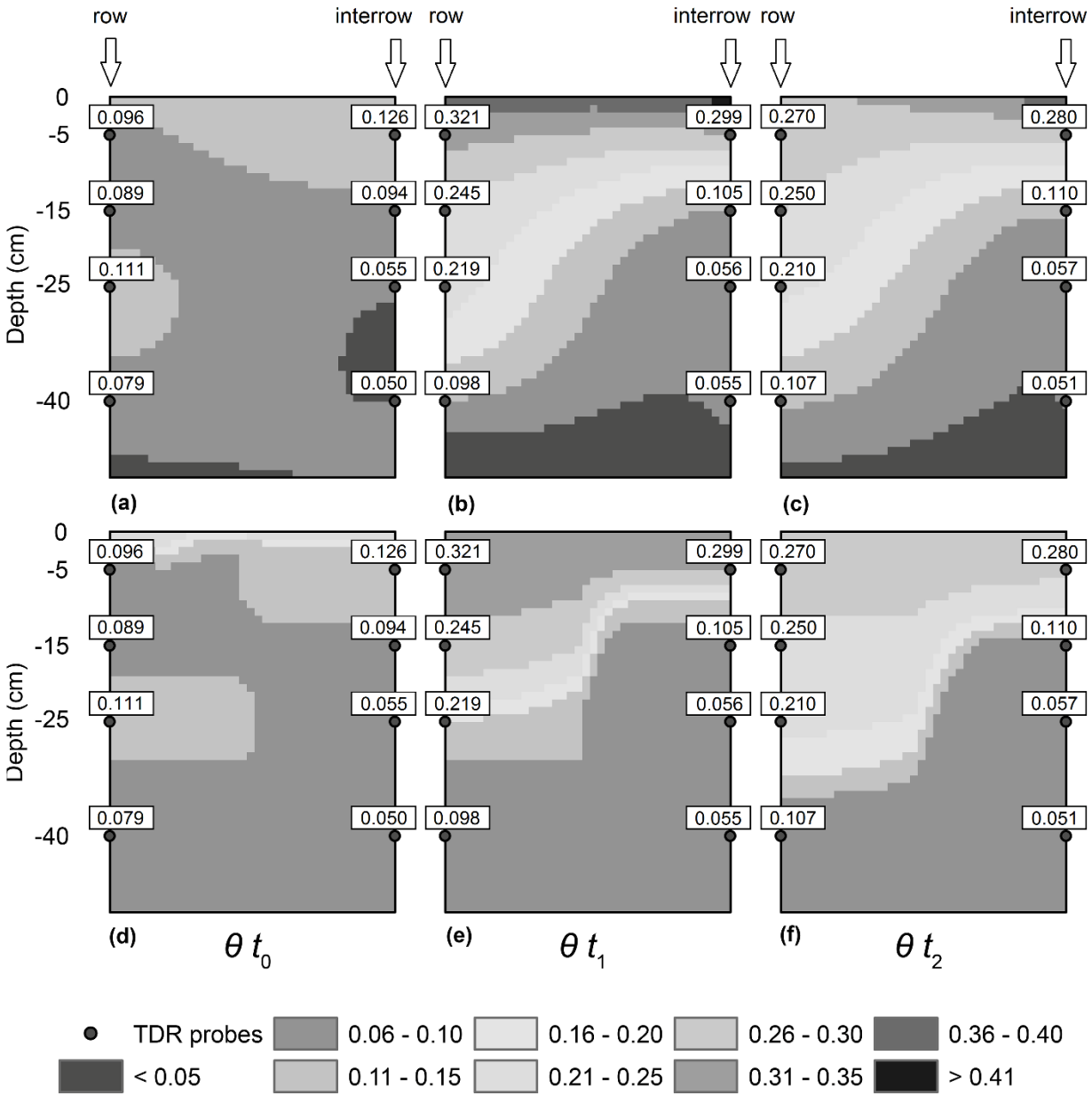
row
interrow
row
interrow
row
interrow
Depth (cm)
0
-5
-15
-25
-40
0.096
0.126
0.089
0.094
0.111
0.055
0.079
0.050
0.321
0.299
0.245
0.105
0.219
0.056
0.098
0.055
0.270
0.280
0.250
0.110
0.210
0.057
0.107
0.051
(a)
(b)
(c)
(d)
θ t0
(e)
θ t1
(f)
θ t2
TDR probes
< 0.05
0.06 - 0.10
0.11 - 0.15
0.16 - 0.20
0.21 - 0.25
0.26 - 0.30
0.31 - 0.35
0.36 - 0.40
> 0.41

Figure 5

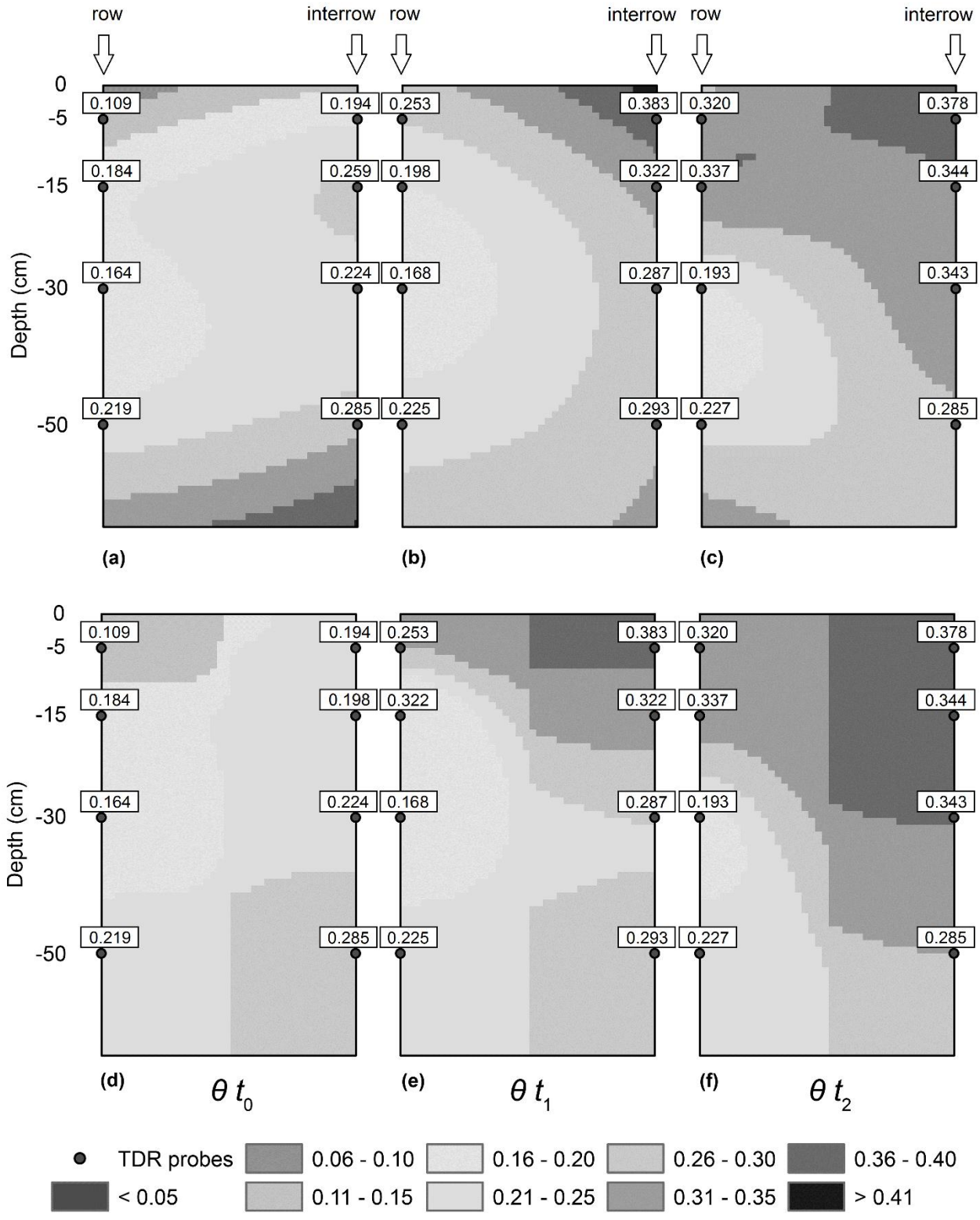
row
interrow
row
interrow
row
interrow
Depth (cm)
0
-5
-15
-30
-50
0.109
0.194
0.253
0.383
0.320
0.378
0.184
0.259
0.198
0.322
0.337
0.344
0.164
0.224
0.168
0.287
0.193
0.343
0.219
0.285
0.225
0.293
0.227
0.285
(a)
(b)
(c)
(d)
θ t0
(e)
θ t1
(f)
θ t2
TDR probes
< 0.05
0.06 - 0.10
0.11 - 0.15
0.16 - 0.20
0.21 - 0.25
0.26 - 0.30
0.31 - 0.35
0.36 - 0.40
> 0.41

Figure 6

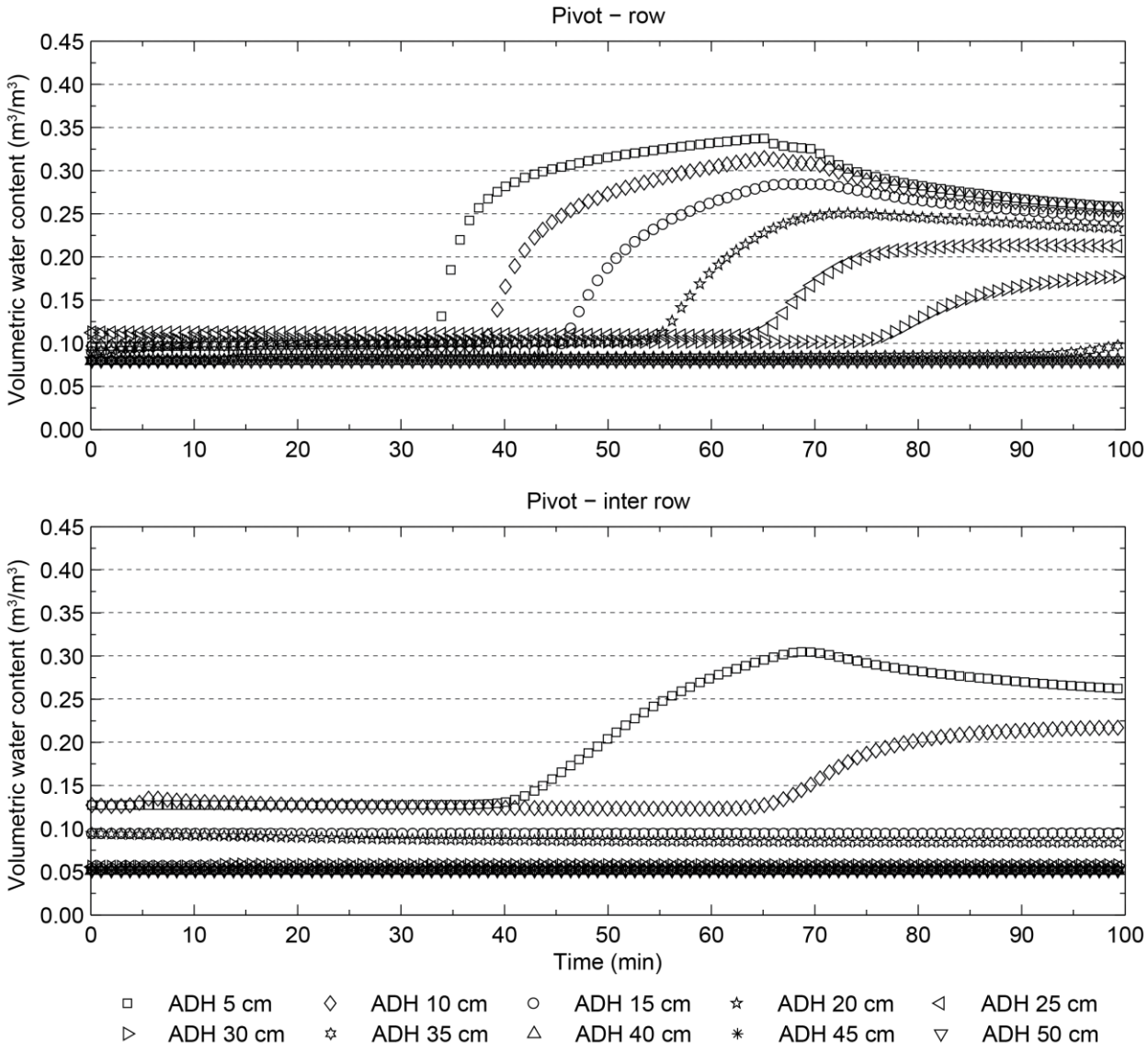
Pivot − row
Volumetric water content (m³/m³)
0.45
0.40
0.35
0.30
0.25
0.20
0.15
0.10
0.05
0.00
0
10
20
30
40
50
60
70
80
90
100
Pivot − inter row
Volumetric water content (m³/m³)
Time (min)
ADH 5 cm
ADH 10 cm
ADH 15 cm
ADH 20 cm
ADH 25 cm
ADH 30 cm
ADH 35 cm
ADH 40 cm
ADH 45 cm
ADH 50 cm

Figure 7

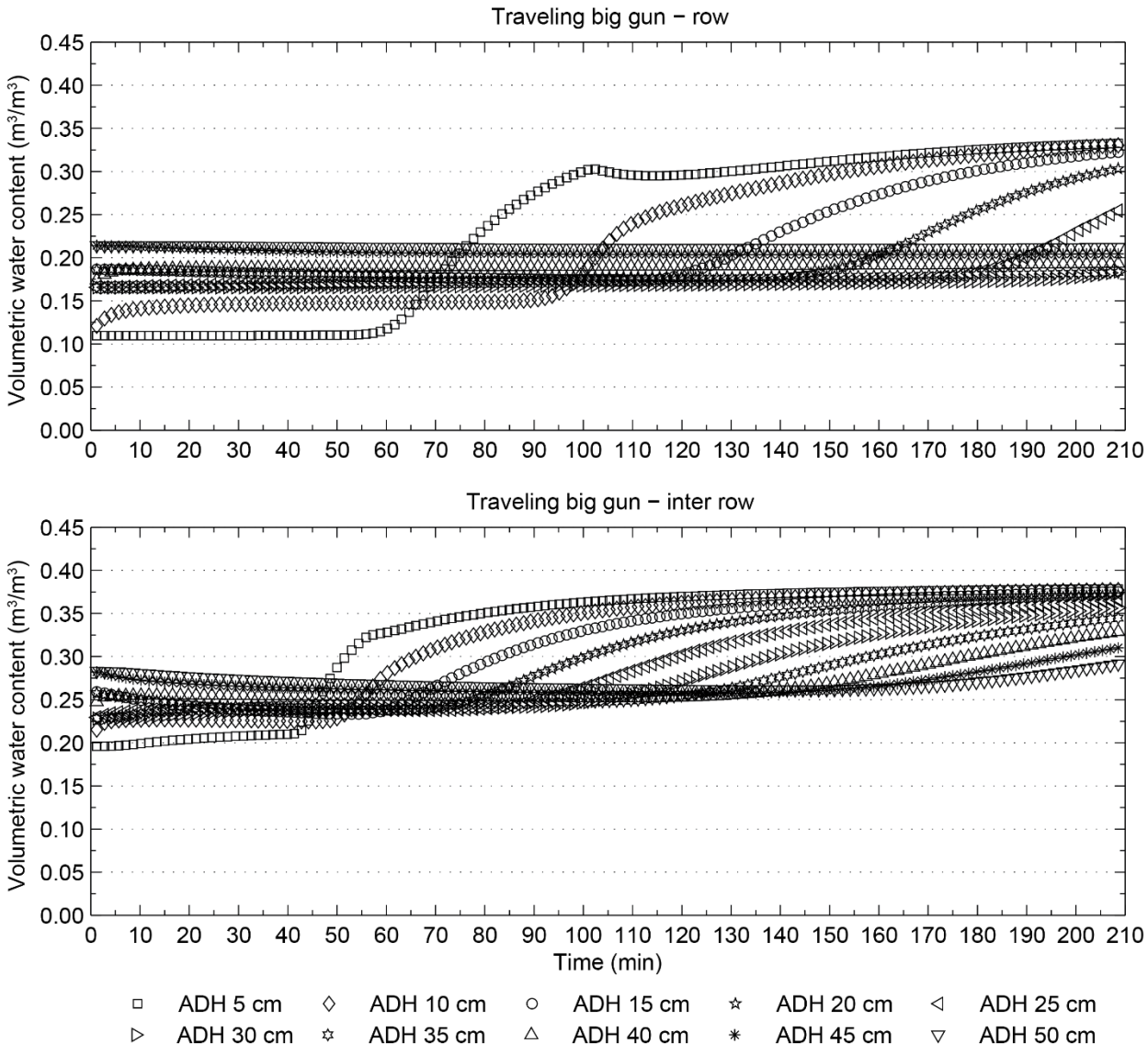
Traveling big gun − row
Volumetric water content (m³/m³)
0.45
0.40
0.35
0.30
0.25
0.20
0.15
0.10
0.05
0.00
0 10 20 30 40 50 60 70 80 90 100 110 120 130 140 150 160 170 180 190 200 210
Traveling big gun − inter row
Volumetric water content (m³/m³)
0.45
0.40
0.35
0.30
0.25
0.20
0.15
0.10
0.05
0.00
0 10 20 30 40 50 60 70 80 90 100 110 120 130 140 150 160 170 180 190 200 210
Time (min)
ADH 5 cm
ADH 10 cm
ADH 15 cm
ADH 20 cm
ADH 25 cm
ADH 30 cm
ADH 35 cm
ADH 40 cm
ADH 45 cm
ADH 50 cm

Figure 8